Published in final edited form as:
Science. 2008 August 15; 321(5891): 964–967. doi:10.1126/science.1159505.

Suppression of the microRNA pathway by bacterial effector proteins

Lionel Navarro[1], **Florence Jay**[1], **Kinya Nomura**[2], **Sheng Yang He**[2], and **Olivier Voinnet**[1,*]

1*Institut de Biologie Moléculaire des Plantes, CNRS UPR2353 -Université Louis Pasteur. 12, rue du Général Zimmer 67084 Strasbourg Cedex, France*

2*Department of Energy Plant Research Laboratory, Michigan State University, East Lansing, MI 48824, USA*

Abstract

Plants and animals sense pathogen-associated molecular patterns (PAMPs) and in turn differentially regulate a subset of microRNAs (miRNAs). However, the extent to which the miRNA pathway contributes to innate immunity remains unknown. Here, we show that miRNA-deficient mutants of Arabidopsis partly restore growth of a type-three secretion-defective mutant of *Pseudomonas syringae*. These mutants also sustained growth of non-pathogenic *Pseudomonas fluorescens* and *Escherichia coli* strains, implicating miRNAs as key components of plant basal defense. Accordingly, we have identified *P. syringae* effectors that suppress transcriptional activation of some PAMP-responsive miRNAs, miRNA biogenesis, stability or activity. These results provide compelling evidence that, like viruses, bacteria have evolved to suppress RNA silencing to cause disease.

In RNA silencing, double-stranded (ds)RNA is processed into small RNAs through the action of RNase-III-like Dicer enzymes. The small RNAs guide Argonaute (AGO)-containing RNA-induced silencing complexes (RISCs) to inhibit gene expression at the transcriptional or post-transcriptional levels (1). In the *Arabidopsis thaliana* miRNA pathway, miRNA precursors (pre-miRNAs) are excised from non-coding primary transcripts (pri-miRNAs) and processed into mature miRNA duplexes by Dicer-like 1 (DCL1). Upon HEN1-catalyzed 2′-O-methylation (2), one miRNA strand incorporates an AGO1-containing RISC to direct endonucleolytic cleavage or translational repression of target transcripts (1). DCL4 and DCL2 have major defensive functions by processing viral-derived dsRNA into small interfering (si) RNAs, which, like miRNAs, are loaded into AGO1-RISC. As a counter-defensive strategy, viruses deploy viral suppressors of RNA-silencing, or VSRs (3). RNA-silencing also contributes to resistance against bacterial pathogens (4-7), which elicit an innate immune response upon perception of PAMPs by host-encoded pattern recognition receptors (PRRs). For example, the Arabidopsis miR393 is PAMP-responsive (4,8) and contributes to resistance against virulent *P. syringae* pv. *tomato* strain DC3000 (*Pto* DC3000) (4). Nonetheless, the full extent to which cellular small RNAs, including miRNAs, participate to PAMP-triggered immunity (PTI) in plants remains unknown.

To address this issue, Arabidopsis mutants defective for siRNA or miRNA accumulation were challenged with *Pto* DC3000 *hrcC*-, a mutant that lacks a functional type-III secretion system required for effector protein delivery into host cells (9). This bacterium elicits, but cannot suppress PTI, and consequently multiplies poorly on wild-type Col-0- and La-*er*-inoculated leaves (Fig. 1A,S1). However, *Pto* DC3000 *hrcC*-growth was specifically enhanced in the

*To whom correspondence should be addressed: olivier.voinnet@ibmp-ulp.u-strasbg.fr

miRNA-deficient *dcl1-9* and *hen1-1* mutants (Fig. 1A), in which induction of the basal defense marker gene *WRKY30* was also compromised ((10), Fig. S2A).

Because PTI is also a major component of non-host resistance (10,11), we challenged *dcl1-9* and *hen1-1* mutants with *P. syringae* pv. *phaseolicola* (*Psp*) strain NPS3121, which infects bean but not Arabidopsis. Both *dcl1-9* and *hen1-1* mutants sustained *Psp* NPS3121 growth (Fig. 1B) and displayed compromised *WRKY30* induction (Fig. S2B). Enhanced bacterial growth was also observed with the non-pathogenic *P. fluorescens* Pf-5 and *E. coli* W3110 strains (Fig. 1C/D). Furthermore, the above non-virulent bacteria all induced chlorosis and necrosis on miRNA-deficient mutants resembling bacterial disease symptoms triggered by virulent *Pto* DC3000 (Fig. 1E,S3A-D). However, we cannot exclude the participation of other endogenous small RNAs in this process (6,7) because the *hen1-1* mutant, which is additionally impaired in the accumulation of many types of small RNAs (12), consistently displayed more disease symptoms than the *dcl1-9* mutant did (Fig. S3). Despite this possibility, our results indicate that the miRNA pathway is likely to be an essential component of plant basal defense. As a corollary, some bacterial effectors must have evolved to suppress host miRNA functions to enable disease.

In principle, suppression of the miRNA pathway could affect miRNA transcription, biogenesis or activity. To test the first possibility, we challenged wild-type plants with *Pto* DC3000 or *Pto* DC3000 *hrcC*-, and analyzed the levels of several pri-miRNAs. In virulent *Pto* DC3000-treated plants, induction of the PAMP-responsive pri-miR393a/b and pri-miR396b (4,8) was significantly suppressed, as was induction of *WRKY30* and *Flagellin Receptor Kinase 1* (*FRK1*) (13) used as internal controls (Fig. 2A). By contrast, the PAMP-insensitive pri-miR166a and pri-miR173 remained unaffected. We then used the previously described miR393a-p::eGFP and miR393b-p::eGFP transgenic lines, which report *miR393a* and *miR393b* transcriptional activity (4). *Pto* DC3000 *hrcC*- caused an increase in eGFP mRNA levels in both transgenic lines, indicating the presence of PAMP-responsive elements upstream of *miR393a* and *miR393b* (Fig. 2B). However, this induction was compromised by *Pto* DC3000, as was induction of the *FRK1* control (Fig. 2B). These results suggest that some *Pto* DC3000 effectors suppress PAMP-triggered transcriptional activation of pri-miR393a/b.

To test this hypothesis, we engineered T-DNA constructs to deliver distinct *Pto* DC3000 effectors into leaves of the Arabidopsis *efr* mutant, which sustains efficient *Agrobacterium*-mediated transient transformation (14) without affecting pri-miRNA, mature miRNA or miRNA target levels (Fig. S4). Bacterial effector expression was confirmed (Fig. S5A), and pri-miRNA levels subsequently monitored. AvrPtoB, an effector with E3-ubiquitin ligase activity (15), down-regulated pri-miR393a and pri-miR393b accumulation without affecting the PAMP-insensitive pri-miR166a (Fig. 2C). This effect occurs, at least in part, at the transcriptional level because AvrPtoB delivery into miR393a-p::eGFP/*efr* and miR393b-p::eGFP/*efr* leaves inhibited both basal expression and PAMP-triggered induction of *eGFP* (Fig. 2E/F,S5B). Similar effects were obtained with $AvrPtoB_{F525A}$, a stable mutant in which the E3-ligase activity is abolished (Fig. 2D-F,S5B). Therefore, AvrPtoB suppresses *miR393a* and *miR393b* transcription independently of its E3-ligase activity, as previously shown for AvrPtoB-mediated suppression of PAMP-responsive *FRK1* (16).

To assay for interference with miRNA biogenesis or stability, levels of several PAMP-insensitive and -sensitive miRNAs were monitored upon transient effector delivery into *efr* leaves. Three bacterial effectors significantly reduced accumulation of unrelated miRNAs (Fig. 3A, S5A-C, S6), among which AvrPto is a well-characterized *Pto* DC3000 effector with demonstrated virulence function ((17), Fig. S9). Further molecular analysis revealed that AvrPto-mediated reduction in miRNA accumulation may occur, at least in part, at the post-transcriptional level because AvrPto did not alter pri-miRNA transcript levels (Fig. S7A).

Accordingly, conditional AvrPto expression in stable transgenic lines stabilizes miR393 precursors and concomitantly decreases accumulation of mature miR393, with no or little effects on pri-miR393 transcript levels (Fig. 3B/C, S7B). Therefore, AvrPto possibly interferes with processing of some miRNA precursors, a phenomenon also observed during *Pto* DC3000 infection (Fig. 3C, S8).

AvrPto interacts with, and inhibits the kinase activity of, multiple transmembrane PRRs (18). Moreover, AvrPto strongly interacts with BAK1 (BRI1-Associated receptor-kinase 1), a shared signaling partner of the brassinosteroid receptor BRI1 (Brassinosteroid-Insenstive 1) and the flagellin receptor FLS2 (Flagellin Sensing 2) (19-21). The AvrPto-BAK1 interaction compromises the ligand-dependent FLS2-BAK1 association resulting in suppression of PTI (19). Accordingly, $AvrPto_{Y89D}$, which is unable to interact with PRRs and BAK1 (18,19), displays compromised virulence function (18). Transient delivery of $AvrPto_{Y89D}$ did not alter miRNA accumulation, nor did delivery of $AvrPto_{G2A}$, carrying a mutated myristoylation site that disrupts AvrPto host plasma membrane localization ((16,22), Fig. 3A, S5C). Conditional expression of an N-terminal histidine-tagged version of AvrPto (6xHis-AvrPto) displaying similarly compromised subcellular localization and virulence function gave comparable results (Fig. 3B/C, S9). We conclude that AvrPto interferes with miRNA accumulation and this interference is linked with its virulence function (SOM text).

Finally, we tested whether *Pto* DC3000 effectors could also suppress miRNA activity. We used the SUC-*SUL* (SS) reporter line in which phloem-specific expression of an inverted-repeat transgene triggers non-cell-autonomous RNAi of the endogenous SULPHUR (SUL) transcript, causing vein-centered chlorosis (23). Of the 21nt (DCL4-dependent) and 24nt (DCL3-dependent) *SUL* siRNA species, only the former is required for RNAi in an AGO1-dependent manner (23). Stable transgenic lines overexpressing HopT1-1 (Fig. S10) exhibited attenuated chlorosis (Fig. 3E) and accumulated higher *SUL* mRNA levels (Fig. 3G). However, the *SUL* siRNA levels remained unchanged (Fig. 3D), mimicking the reported effects of the *ago1-12* mutation in SS (23). Also as in *ago1-12*, canonical miRNAs accumulated normally in HopT1-1-overexpressing lines, despite higher levels of miRNA target transcripts (Fig. 3F/G,S11) suggesting that HopT1-1 likely suppresses slicing mediated by AGO1. Interestingly, further transient overexpression of HopT1-1 in *efr* plants showed a dramatic increase in the protein, but not mRNA, levels of the miR834 target COP1-interacting protein 4 (CIP4) (Fig. 3H,S12A/B). Thus, HopT1-1 additionally, and perhaps predominantly, suppresses miRNA-directed translational inhibition, which is consistent with the involvement of AGO1 in this second process (24). Similarly, higher protein levels of CIP4 and of the copper/zinc superoxide dismutase 1 (CSD1-miR398 target) were detected in plants infected with virulent *Pto* DC3000 (Fig. 3H, S12C), with no effect on CSD1, CIP4 and some other miRNA target transcript levels (Fig. S13).

We show here that the miRNA pathway plays a major role in antibacterial basal defense and, accordingly, we have identified bacterial suppressors of RNA silencing or 'BSRs'. This finding provides a plausible explanation for the synergistic interactions observed in the field between some viral and bacterial phytopathogens. Consistent with this idea, we found that infection by *Turnip Mosaic Virus* (TuMV), which produces the P1-HcPro suppressor of siRNA and miRNA functions (25,26) reduces basal and non-host resistances to promote growth and disease-like symptoms from non-virulent *Pto* DC3000 *hrcC*- and *Psp* NPS3121 bacteria (Fig. 4). It will now be important to elucidate how silencing factors are modified by VSRs and BSRs, and whether such modifications are sensed by specific Resistance (R) proteins, as postulated by the 'guard hypothesis' (27).

The implication of the miRNA pathway in innate immunity is not specific to plants. For example, human *MiR146* is induced by several microbial components (28). Because type III

secretion systems are widespread across Gram-negative bacteria (29), the intriguing possibility emerges that human pathogenic bacteria also have evolved to suppress RNA silencing to cause disease.

Supplementary Material

Refer to Web version on PubMed Central for supplementary material.

Acknowledgements

We thank Y. Yamamoto, A. Collmer, J. Alfano, G. Martin, C. Zipfel, E. Cascales, G. Preston, P. Hauck and Y. B. Kwack for materials. Supported by a Fellowship from the Federation of European Biochemical Societies (L.N); an Action Thématique Incitative sur Programme grant from the CNRS and a grant from the trilateral génoplante–German Plant Genome Research Program–Spanish ministry of Research (F.J and O.V); and US NIH grant #5R01AI060761 (K.N and SY.H).

References

1. Baulcombe D. Nature 2004;431:356. [PubMed: 15372043]
2. Yu B, et al. Science 2005;307:932. [PubMed: 15705854]
3. Ding SW, Voinnet O. Cell 2007;130:413. [PubMed: 17693253]
4. Navarro L, et al. Science 2006;312:436. [PubMed: 16627744]
5. Katiyar-Agarwal S, et al. Proc Natl Acad Sci U S A 2006;103:18002. [PubMed: 17071740]
6. Agorio A, Vera P. Plant Cell 2007;19:3778. [PubMed: 17993621]
7. Katiyar-Agarwal S, Gao S, Vivian-Smith A, Jin H. Genes Dev 2007;21:3123. [PubMed: 18003861]
8. Fahlgren N, et al. PLoS ONE 2007;2:e219. [PubMed: 17299599]
9. Yuan J, He SY. J Bacteriol 1996;178:6399. [PubMed: 8892851]
10. Li X, et al. Proc Natl Acad Sci U S A 2005;102:12990. [PubMed: 16123135]
11. de Torres M, et al. Plant J 2006;47:368. [PubMed: 16792692]
12. Li J, Yang Z, Yu B, Liu J, Chen X. Curr Biol 2005;15:1501. [PubMed: 16111943]
13. Asai T, et al. Nature 2002;415:977. [PubMed: 11875555]
14. Zipfel C, et al. Cell 2006;125:749. [PubMed: 16713565]
15. Janjusevic R, Abramovitch RB, Martin GB, Stebbins CE. Science 2006;311:222. [PubMed: 16373536]
16. He P, et al. Cell 2006;125:563. [PubMed: 16678099]
17. Hauck P, Thilmony R, He SY. Proc Natl Acad Sci U S A 2003;100:8577. [PubMed: 12817082]
18. Xiang T, et al. Curr Biol 2008;18:74. [PubMed: 18158241]
19. Shan L, et al. Cell Host Microbe 2008;4:17. [PubMed: 18621007]
20. Chinchilla D, et al. Nature 2007;448:497. [PubMed: 17625569]
21. Li J, et al. Cell 2002;110:213. [PubMed: 12150929]
22. Shan L, Thara VK, Martin GB, Zhou JM, Tang X. Plant Cell 2000;12:2323. [PubMed: 11148281]
23. Dunoyer P, Himber C, Ruiz-Ferrer V, Alioua A, Voinnet O. Nat Genet 2007;39:848. [PubMed: 17558406]
24. Brodersen P, et al. Science 2008;320:1185. [PubMed: 18483398]
25. Kasschau KD, Carrington JC. Cell 1998;95:461. [PubMed: 9827799]
26. Kasschau KD, et al. Dev Cell 2003;4:205. [PubMed: 12586064]
27. Dangl JL, Jones JD. Nature 2001;411:826. [PubMed: 11459065]
28. Taganov KD, Boldin MP, Chang KJ, Baltimore D. Proc Natl Acad Sci U S A 2006;103:12481. [PubMed: 16885212]
29. Mota LJ, Cornelis GR. Ann Med 2005;37:234. [PubMed: 16019722]

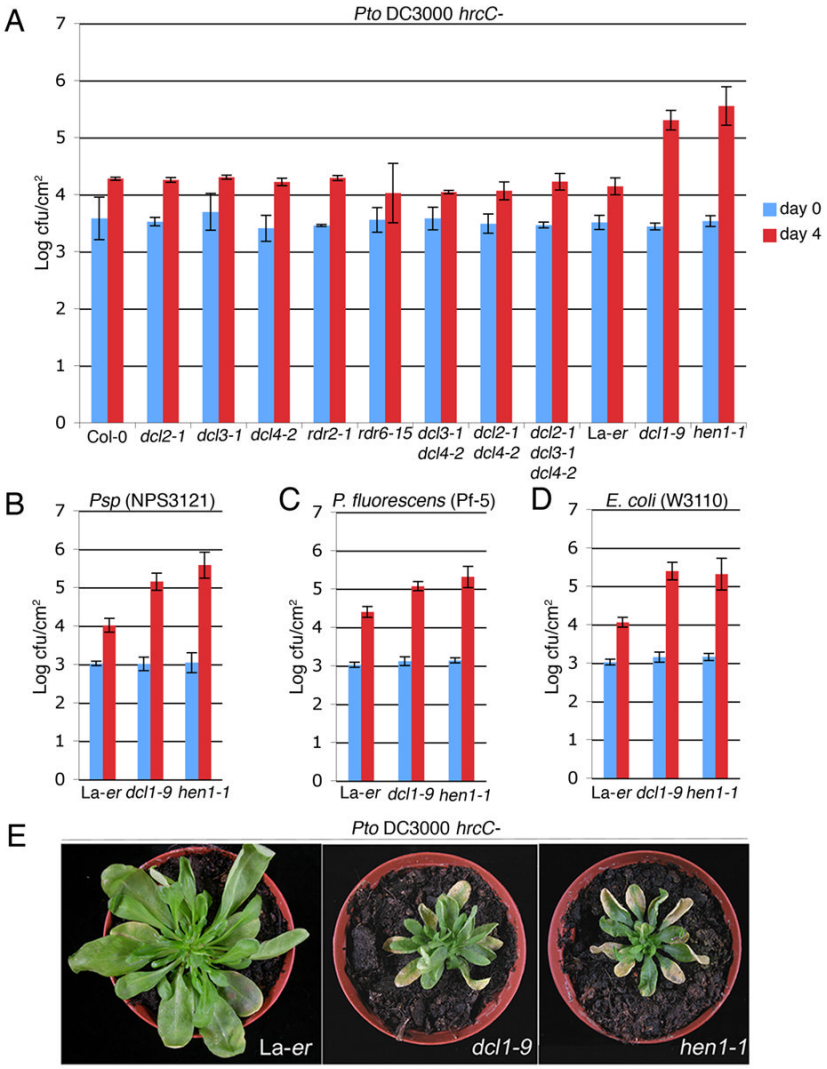

Fig. 1.

The Arabidopsis miRNA pathway promotes basal and non-host resistances to bacteria. (A) Six-week-old plants were inoculated by syringe-infiltration using a *Pto* DC3000 *hrcC*- concentration of 10^6 colony-forming units (cfu) per ml. Error bars: standard error of log-transformed data from five independent samples. Similar results were obtained in three independent experiments. (B-D) Plants were inoculated as in (A), but with *Psp* NPS3121. (B), *P. fluorescens* Pf-5 (C) or *E. coli* W3110 (D). Similar results were obtained in two independent experiments. (E) Plants were inoculated as in (A) and picture taken at 6 days post-inoculation (dpi).

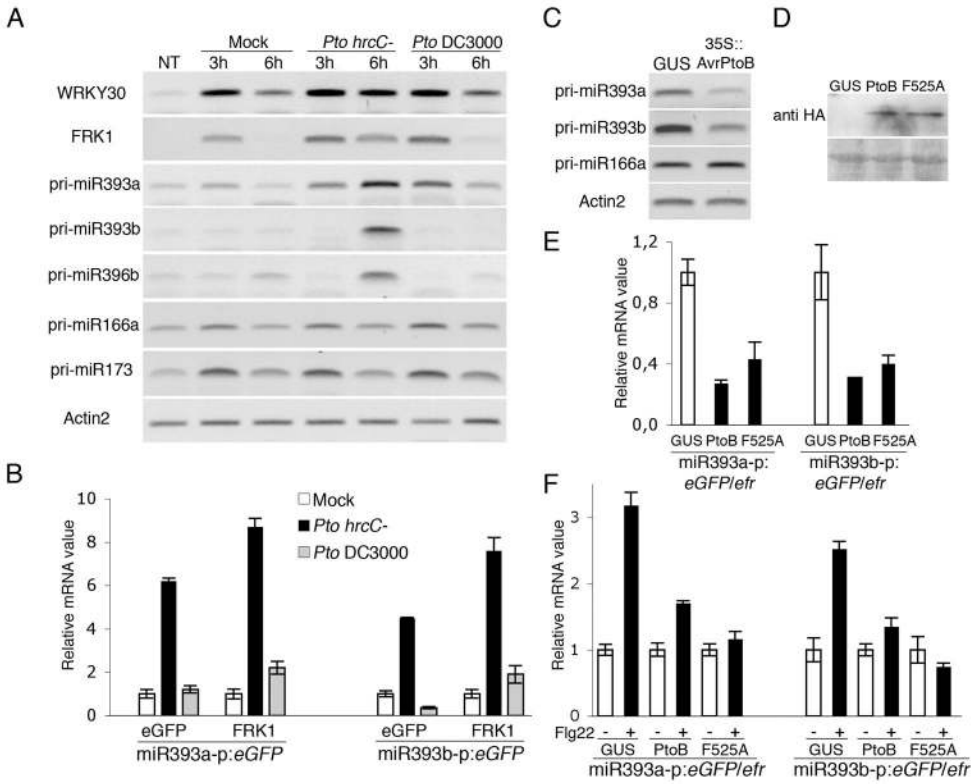

Fig. 2.

Transcriptional repression of PAMP-responsive miRNAs by *Pto* DC3000 and AvrPtoB. (A) Five-week-old plants were syringe-infiltrated with a concentration of 2×10^7 cfu/ml of either *Pto* DC3000 or *Pto* DC3000 *hrcC*- and pri-miRNA expression monitored by semi-quantitative RT-PCR. Similar results were obtained in three independent experiments. (B) Five-week-old miR393a-p::eGFP and miR393b-p::eGFP transgenic lines were treated as in (A) for 6 hours. eGFP and FRK1 mRNA levels were analyzed by qRT-PCR. Similar results were obtained in three independent experiments. (C) Semi-quantitative RT-PCR analysis of pri-miRNAs. *Agrobacterium*-mediated transient expression was performed in four-week-old *efr* leaves. Similar results were obtained in three independent experiments. (D) Detection of AvrPtoB-3xHA and $AvrPtoB_{F525A}$-3xHA by Western analysis. Bottom panel: coomassie staining shows equal protein loading. Transient expression was performed as in (C). (E) Transient expression was performed in 4-week-old miR393a-p::eGFP/*efr* and miR393b-p::eGFP/*efr* lines as in (C). Expression of eGFP was monitored by qRT-PCR. (F) As in (E) except that 3 days-post *Agrobacterium*-infiltration, plants were challenged with 1μM of active or inactive flg22 for 6 hours.

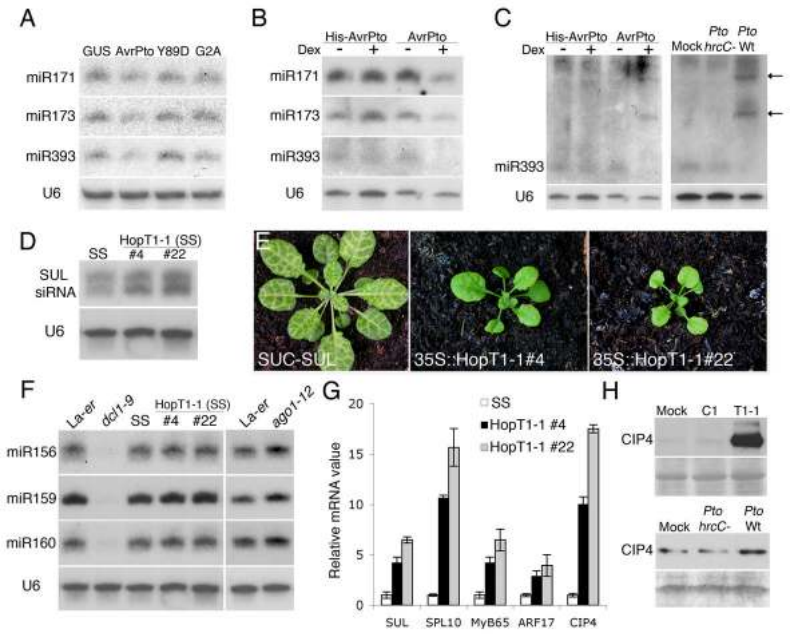

Fig. 3.

Suppression of miRNA accumulation or activity by bacterial effectors. (A). Four-week-old *efr* plants were syringe-infiltrated with *A. tumefaciens* carrying AvrPto, AvrPto$_{Y89D}$, AvrPto$_{G2A}$ or GUS-intron (GUS) constructs. Five days post-infiltration, accumulation of miRNAs was assayed by Northern analysis. U6: control shows small RNA equal loading. Similar results were obtained in two independent experiments. (B) Same experiments as in (A), but in Dex::AvrPto and Dex::6xHis-AvrPto transgenic lines. MiRNA accumulation was analyzed by Northern analysis 30 hours after dexamethasone (Dex) treatment (at a concentration of 30 μM). Similar results were obtained in two independent experiments (C) Left panel: as in (B) on miR393. Right panel: Five-week-old Col-0 plants were syringe-infiltrated with 10^8 cfu/ml of *Pto* DC3000 *hrcC*- or *Pto* DC3000 and miRNA levels analyzed at 30 hpi (pre-miRNA stabilization was detected by 24 hpi). Similar results were obtained in five independent experiments. Arrows: miR393 precursors. (D) Northern analysis of SUL siRNA levels in SUC-*SUL* (SS) plants overexpressing HopT1-1. (F) Northern analysis of canonical miRNA levels in HopT1-1-overexpressing (SS) plants. (G) qRT-PCR analysis of SUL and miRNA target transcript levels in HopT1-1-overexpressing (SS) plants. (H) HopT1-1 and Pto DC3000 elevate CIP4 protein levels. Upper panels: Transient expression of HopT1-1 (T1) or HopC1 (C1) in 4-week-old *efr* leaves. CIP4 protein levels were analyzed by Western analysis using an anti CIP4 antibody. Ponceau staining shows equal protein loading. Bottom panels: Five-week-old Col-0 plants were syringe-infiltrated with *Pto* DC3000 or *Pto* DC3000 *hrcC*- at 10^8 cfu/ml and CIP4 protein levels analyzed at 6 hpi. Coomassie staining shows equal protein loading. Similar results were obtained in two independent experiments.

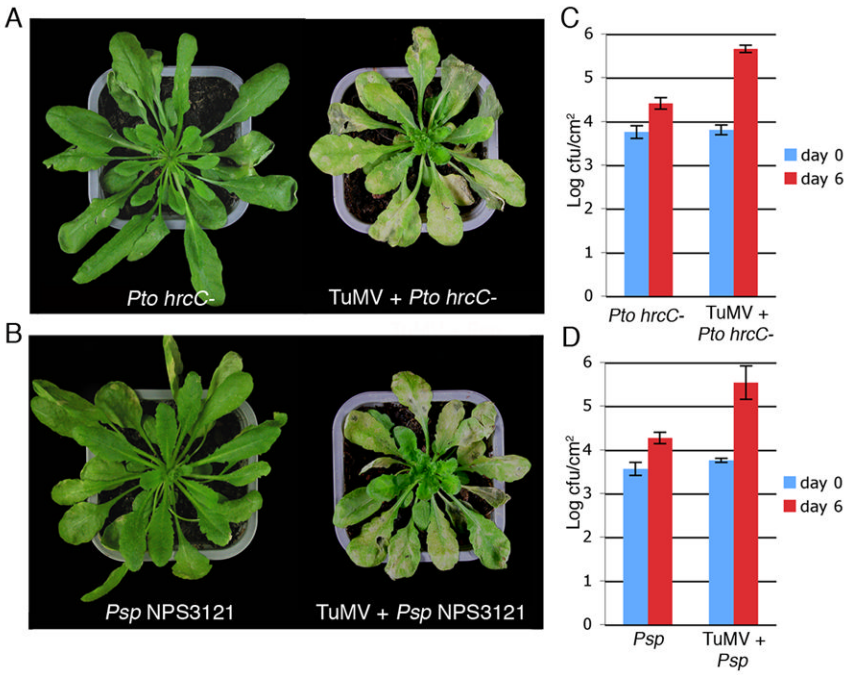

Fig. 4.

TuMV infection enhances growth of and rescues symptoms induced by *Pto* DC3000 *hrcC*- and *Psp* NPS3121. (A) Five-week-old Col-0 plants were infected for 7 days with TuMV and further challenged with *Pto* DC3000 *hrcC*- at a concentration of 10^6 cfu/ml. The picture was taken 5 days post-bacterial infiltration. (B). Same as in (A) but with *Psp* NPS3121. (C) Growth of *Pto* DC3000 *hrcC*- in mock-inoculated or TuMV-infected Col-0 plants 6 days post-bacterial injection. Error bars: standard error of log-transformed data from five independent samples. Similar results were obtained in two independent experiments. (D) Same as in (C) but with *Psp* NPS3121.